

FABRICATION OF CARBON NANOTUBES ON INTER-DIGITATED METAL ELECTRODE FOR SWITCHABLE NANOPHOTONIC DEVICES

Q. Dai¹, H. Butt¹, R. Rajasekharan¹, T. D. Wilkinson^{1,*}, and G. A. J. Amaratunga^{1,2}

¹Department of Engineering, University of Cambridge, Cambridge, CB3 0FA, UK

²Sri Lanka Institute of Nanotechnology (SLINTEC), Lot 14, Zone A, EPZ, Biyagama, Sri Lanka

Abstract—This paper reports the modeling and characterization of interdigitated rows of carbon nanotube electrodes used to address a liquid crystal media. Finite Element Method modeling of the nanotube arrays was performed to analyze the static electric fields produced to find suitable electrode geometry. A device was fabricated based on the simulation results and electro optics characteristics of the device are presented. This finding has applications in the development of micron and submicron pixels, precise beam steering and nanotube based active back planes.

1. INTRODUCTION

Multiwalled carbon nanotubes (MWCNTs) are promising nanomaterials known for their interesting electrical properties [1]. MWCNTs are mostly metallic and are able to carry high current densities. Due to their high conductivities and aspect ratios they produce very strong electric fields [2, 3]. Myriad research has been dedicated towards utilizing MWCNTs as electrodes in applications like field emission displays [4], rectifiers and other electrical devices [5]. Our group has recently reported the utilization of carbon nanotubes as electrodes to address liquid crystals (LCs) layer [6, 7]. Through this hybrid integration, we have demonstrated novel nanophotonics devices displaying micron-scaled lensing [8], optical modulation and grating effects [9].

Received 26 February 2012, Accepted 2 April 2012, Scheduled 10 April 2012

* Corresponding author: Timothy D. Wilkinson (tdw13@cam.ac.uk).

In these nanophotonic devices, the periodic arrays of vertically aligned carbon nanotubes electrodes are used to form defects in the liquid crystal layer, which then can be manipulated by applying an external electric field. This technology offers completely new ways of controlling liquid crystals molecules, allowing the molecules to move in a variety of directions to create optical components such as nanophotonic lens array. The electric fields produced by the MWCNTs have a Gaussian like profile [2]. LC molecules align parallel to the spawned electric field, producing a three dimensional graded index optical structure which can be used for optical lensing and phase modulation.

Previously we used MWCNT arrays with lattice constants of $10\ \mu\text{m}$ and tube heights around $5\ \mu\text{m}$ to fabricate the nanophotonic lens array [6]. Around each nanotube a 3D defect is produced (in the LC layer) which acts as a lens. By using carbon nanotubes as electrodes, the liquid crystals layers can be addressed at micro-scales and high resolution pixels can be produced. However, for applications like optical beam steering, holography, micron and sub micron pixel development the nanotube electrodes need to be switched at different voltages. In this paper, we present a new geometry for the LC and MWCNT based device where we use interdigitated rows of MWCNT arrays to address a liquid crystal medium with the capability of applying different voltages to the interdigitated electrodes (alternating rows of CNT arrays) and the common ground plane. In the previous devices, all the CNT arrays were attached to the lower electrode and placed at the same electric potential [6, 7]. The current geometry is more desirable and first step for developing sub-micron pixels, nanophotonic beam steering and nanotube based backplane. For this purpose the CNTs were grown on patterned interdigitated metal electrodes. CNT growth on metal masks was one of the toughest challenges which we overcame. Our electromagnetic simulation results suggest that by applying different potentials on alternative CNT rows, more complex electric field profiles can be produced (within the LC layer) for realizing different optical elements in the liquid crystal layer.

2. ELECTROMAGNETIC SIMULATION OF THE CNT ELECTRODE GEOMETRY

Finite Element Method (FEM) modeling of CNT arrays was performed to characterize the static electric fields produced in the nanophotonic device. We studied the new geometry for the hybrid LC and CNT devices where their individual optical function can be modified electrically. Unlike previous devices where all the CNTs were placed

at the same electric potential [7], different potentials can be applied to each row CNT array to produce a more complex electric field profile suiting more complex optical requirements of certain applications.

The modeling of the electrical field effects of carbon nanotubes was carried out using COMSOL Multiphysics [10], a finite element method (FEM) based modeling software package. The CNTs were modeled as perfect electric conductor (PEC) rods of nanometer dimensions in vacuum for micro-scale device cells with the geometry as shown in Figure 1(a). Rows of carbon nanotubes with a 50 nm radius, height of 2 μm and interspacing of 1 μm were modeled. Each row was attached to a separate planar metallic conductor so that a separate voltage can be applied to it. The top electrode plate was set to ground. The lateral boundaries of the geometry were set to a symmetric boundary condition.

The electrostatic electric fields were computed using COMSOL ELECTROSTATICS MODULE. The Laplace's equation for the scalar potential V , given by $-\nabla \cdot (\epsilon \nabla V) = 0$, was solved over the device geometry. Later the electric fields \vec{E} produced by the CNTs rows were computed by taking the gradient of the calculated potential

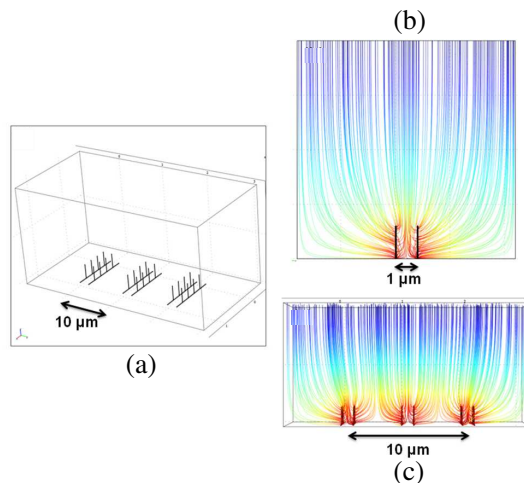


Figure 1. Modelled geomerty of CNTs in vacumm. Each row of CNTs is connected to a different metallic row. All the metallic rows were placed at a potential of 5 volts. The top planar electrode was set to ground. (b) 2D view of the static electric field produced by a pair of CNTs rows. (c) The same for three pair of rows. Each pair produces a near gaussian like field profile which can be used to address LCs.

$\vec{E} = -\nabla V$, over the model. Figures 1(b)–(c) show the simulated results for a common potential of 5 volts applied to all the carbon nanotube rows. The CNTs arrays act as the common bottom electrode in this arrangement. The resultant electric fields mostly extend vertically from the bottom CNT electrode to the top ground electrode. The presence of CNTs distorts the otherwise constant electric field between the planar top and bottom electrodes. The effective electric field profile produced around each nanotube is Gaussian in nature [6], displaying the highest field intensity above CNT tips. In the LC based nanophotonic device, in response to this electric field profile the liquid crystal molecules would align parallel to the electric field lines (assuming positive anisotropy) producing graded refractive index structures around the carbon nanotubes. Due to a net Gaussian profile these structures act as lenses with focal lengths of the order few tens of microns. The carbon nanotube arrays in this arrangement can be used for producing microlens arrays. The in-depth characterization of such microlenses has been published in our previous papers [8, 11].

In contrast to applying a common potential to the entire nanotubes array, a different potential can be applied to the adjacent rows of carbon nanotubes to produce effectively different electric field profiles. Each row of CNTs is connected to a separate metal electrode and therefore it can be placed at a different electric potential. Figure 2 shows the simulated electric field profiles produced by the CNT rows placed at different electric potentials. In this arrangement a radically curved electric field profile is produced between the CNT rows. Figure 2(b) shows a more detailed view of the electric fields produced between two oppositely polarized CNTs. Such complex

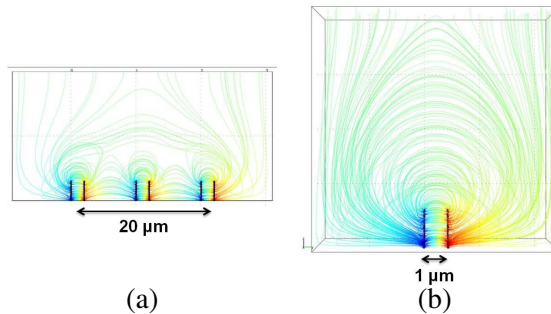


Figure 2. (a) Modeled electric field for a cell containing oppositely polarized CNT rows. (b) The cross-section view of two oppositely polarized rows. The CNTs on right is on -5 volts and left CNT is on 5 volts of potential. Top electrode is set to ground.

electric field profile can be used for realizing micron and submicron scaled pixels, precise beam steering applications and nanotube based active back plane.

At the center of the CNT rows, due to an average horizontal electric field, the LC will be aligned horizontally in the nanophotonic devices creating a high refractive index region. At the edges the LC will obtain, on average, a vertical orientation creating areas with relatively lower refractive index. According to the principle of Fermat, light waves always propagate towards the regions of larger refractive index [12, 13] and the refractive index seen by an incident planar light wave increases towards the center of the rows. The wavefront of the incident light will be focused towards the center of the cell. The strong electric fields produced by the CNTs (on application of small voltages) will make this LC lens very power efficient. By changing the potentials applied on the CNTs and the ground electrode, the depth of the curved electric field profile can be varied.

3. PROPOSED DEVICE GEOMETRY

Innovative fabrication methods are required for the fabrication of the proposed CNT electrode geometry. Each CNT row must have a different base electrode so that a different potential can be applied to it. Nano-scaled electrodes were utilized for this purpose similar to those used in Liquid Crystals over Silicon (LCoS) devices. A schematic diagram of nano-scaled electrodes connected in an interdigitated manner is shown in Figure 3. CNTs can be grown on these interdigitated electrodes. The electric potential applied to the alternative CNT rows can be controlled which effectively produces different electric field profiles within the LC layer.

4. FABRICATION PROCESS

To produce new electrode geometry, firstly the designed interdigitated electrodes were patterned on a silicon dioxide substrate using electron beam (E-beam) lithography. The designed pattern is displayed in Figure 4(a). Then a 150 nm thick layer of tungsten was deposited on the pattern. Plasma enhanced chemical vapor deposition (PECVD) process [2] was used for the growth of CNTs. Several challenges were encountered during the fabrication as discuss in the following paragraphs.

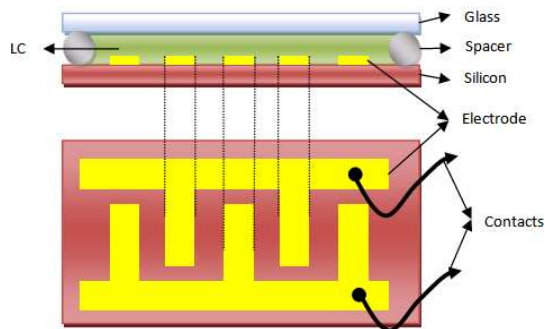


Figure 3. Schematic diagram showing the side and top view of nano-scaled interdigitated electrodes in a liquid crystal cell.

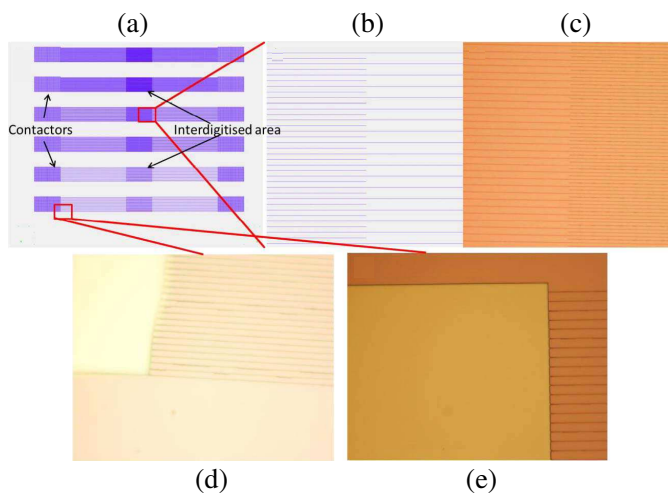


Figure 4. (a) Overview of the interdigitated patterns designed in AutoCAD, there were 6 blocks and the electrodes spacing were $1\ \mu\text{m}$ to $10\ \mu\text{m}$ from top to the bottom, (b) magnified image of overlap area of the interdigitated circuit, (c) microscope image of the pattern produced by UV3, (d) microscope image of the over-exposed pattern using dose 0.8, (e) pattern produced using optimized recipe (dose = 0.7).

4.1. E-beam Lithography Optimization

Polymethyl methacrylate (PMMA) is a widely used conventional photo-resist to accurately produce patterns with sub-micron size features. However, the time required for performing the lithography

of PMMA increases exponentially as the pattern area become larger. For the subject device, the areas of target pattern were over 5 mm^2 and it could take more than 10 hours to pattern the PMMA, which become an obstacle in fabrication. Therefore, UV3 photo-resist was a better choice for the patterning of our application as it provided 10 times faster lithography speed. This allowed the lithography process to be completed in 20 minutes. Substantial parametric optimization was required for UV3 patterning, as the writing dose had to be considerably reduced. Moreover, UV3 is high sensitive photo-resist and the patterns were easily over exposed even with a slight change (by 0.1) in the dose value. For instance, the patterns generated using dose values of 0.8 and 0.7 separately, are displayed in 4(d) & (e). It can be observed that the pattern with a higher dose value was over exposed. After a series of tests, the optimized electron beam lithography recipe was accomplished.

The substrate was prepared by first spin coating UV3 resist for 30 seconds at 5000 rpm. Then a pre-write baking was performed for 1 minute at 120°C . Patterning was done using electron beam lithography with doses of 0.7 and electron beam current of 0.6 nA. After a post-write bake of 2 minutes at 140°C , the substrate was developed (for 2 minutes) in a solution having distilled water to CD-26 ratio of 3 : 1. As shown in Figures 4(c), (e), the interdigitated electrodes were produced accurately in a reduced lithography time of less than 20 minutes.

4.2. Catalyst Deposition for CNT Growth

An optimized combination of catalysts was used for fabricating CNTs on metal substrate. Firstly a 10 nm Al layer was deposited on top of the electrodes as a diffusion layer and then 7 nm of Ni catalyst layer. CNT growth was performed using the conventional plasma enhanced chemical vapour deposition (PECVD) process [6]. The sample was heated up to 800°C and then pre-treatment using NH_3 gas (200 sccm) was carried out for 60 seconds to anneal the catalyst. After that, the plasma was ignited by applying a voltage (640 V) between the grounded stage and the showerhead with a $\text{NH}_3/\text{C}_2\text{H}_2$ (200/50 sccm) gas mixture pumped in at a pressure of 3.1 mbar for 25–30 minutes. This gave rise to the MWCNT growth as shown in Figure 5, allowing maximum heights of around $5 \mu\text{m}$. The amorphous carbon deposited during the CNT growth process was removed by post-treatment, placing the sample in a furnace heated to 500°C for 30 minutes in air.

It was observed that CNTs were not grown on the interdigitated electrodes but rather on the SiO_2 substrate as shown in Figures 5(a), (b). Two possible explanations were concluded for this mal-

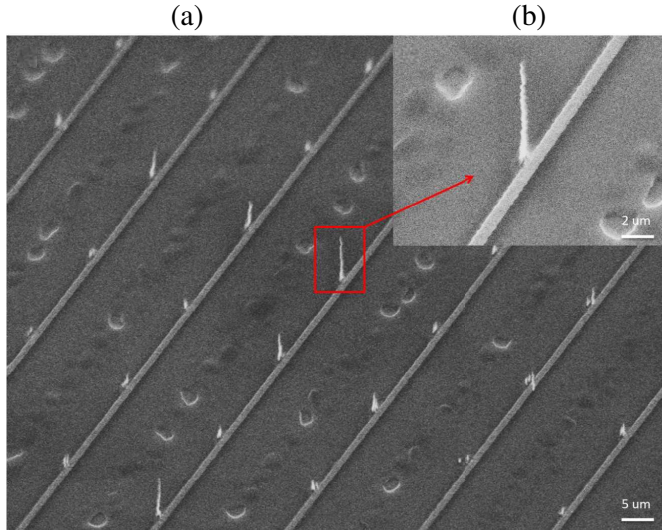


Figure 5. (a) CNTs grown on the tungsten electrodes using standard recipe, (b) magnified image. The CNTs in the red circle were grown on both sides of the electrodes.

function. One was the registration error of the E-beam lithography. A multilayer writing technique was employed to fabricate this sample, in which first the writing was drawn for the interdigitated electrodes as well as the registration mark used for alignment in the later lithography. The second writing was to prepare the catalyst dot arrays for the CNT growth. Slight misalignments may have been involved during the registration process before the second lithography, which then lead to the off growth of CNT. The other possible explanation is that the catalyst dots melted as the temperature increased and slipped to the sides, especially when the width of the electrodes was ~ 150 nm.

Most of CNTs were located at the left side of the tungsten electrodes, but the CNTs highlighted by the red circle were located on both sides (see Figure 5(a)), which suggested that the catalyst dots melting was a more probable causing. To counter this deposition, catalyst thickness was reduced from 7 nm to 5 nm and the pre-growth etching time was also limited to 15 seconds. The successfully grown CNTs on the metal electrodes are shown in Figure 6. CNTs displayed in Figure 6(a) are in the form of vertically aligned forests. The magnified scanning electron microscope (SEM) image in Figure 6(b)) confirmed that the CNTs were precisely grown on the tungsten electrodes, which satisfied the requirements of the interdigitated circuit design.

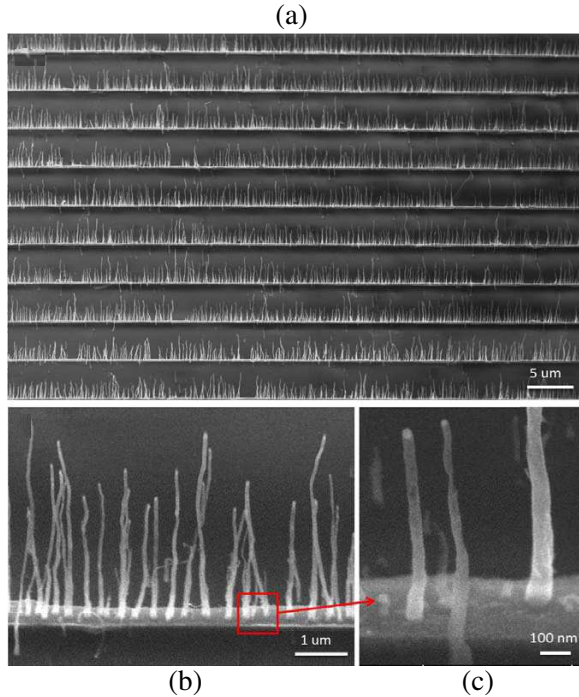


Figure 6. CNTs grown on the tungsten electrodes using optimized recipe, (a) forest CNTs on tungsten electrodes, (b) magnified image, (c) magnified image to prove CNTs were fabricated on the tungsten electrodes.

5. ELECTRO-OPTIC ANALYSIS

A hybrid device was fabricated using the interdigitated carbon nanotube electrodes and nematic liquid crystal as shown in Figure 7. The bottom substrate of the device consists of interdigitated tungsten electrodes (having CNT forests on top as shown in Figure 6) with different spacing. The bottom electrode was assembled with a top electrode (consisting of a layer of indium tin oxide on 0.5 mm thick borosilicate glass) to form the nanophotonic device. The top electrode was given a planar alignment for liquid crystals (to align the LC molecules horizontally) by spin-coating and rubbing a thin film of polyimide (AM4276, Merck). A 20 μm cell gap between substrates was set by silica spacer beads in UV-curing adhesive, and the cell was then filled with a nematic liquid crystal (BL048, Merck), as shown in Figure 7.

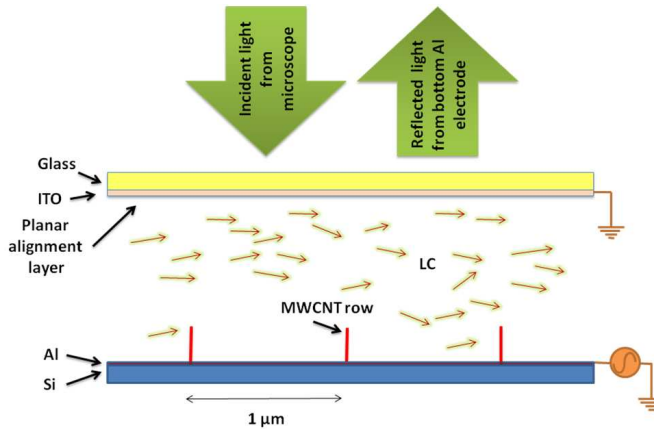


Figure 7. Schematic diagram of the fabricated electro-optical device. Top transparent electrode consisted of ITO on glass and a planar alignment layer for LC. The bottom electrode consisted of row of random CNT arrays on tungsten. The device was analyzed under the optical microscope. The incident light from the top was reflected from the bottom Al layer.

The optical characterization of this was carried out under a polarized optical microscope (OLYMPUS BH2). The polarizer and analyzer were crossed in the experiment. Figures 8(a)–(h) show the device switching at different voltage (magnification $\times 20$). It is well clear that nanotubes interact with liquid crystal and affects the planar alignment around the nanotube [14]. This is the reason the liquid crystal just around the interdigitated electrodes showed a different color compared to dark color of the liquid crystal without any nanotube electrodes between crossed polarizer and analyzer at 0 Vrms as shown in Figure 8(a).

The switching characteristics were studied by applying different voltages to the device. The voltage was applied in such a way that one of the interdigitated electrodes and top electrode was grounded with respect to the other interdigitated electrode. It was observed that the color changed in the positions where the nanotube electrodes present. The color changes in the regions where carbon nanotubes fabricated was different compared to the surrounding liquid crystal medium at different voltages as shown in Figures 8(b)–(h). This shows that the phase modulation of the liquid crystal is different in the nanotube electrodes site and surrounding liquid crystal medium. A defect line also observed in the device when the device started switching. This

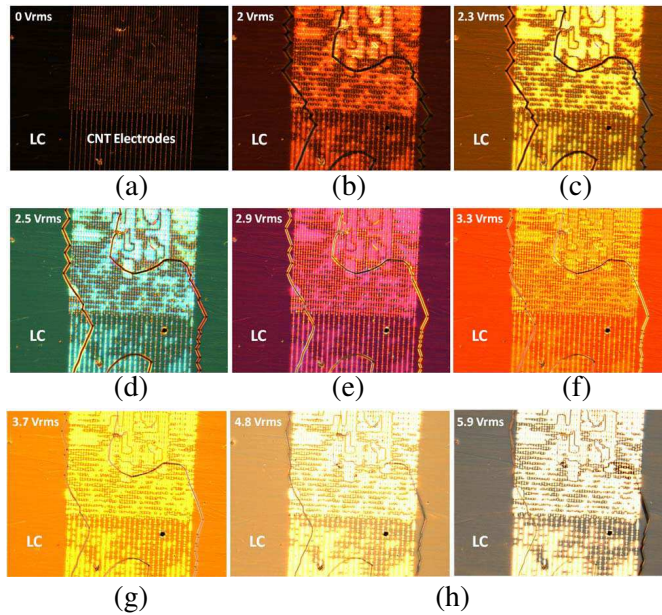


Figure 8. The microscope image of the device between crossed polarizer and analyzer switching at (a) 0 Vrms, (b) 2 Vrm, (c) 2.3 Vrms, (d) 2.5 Vrms, (e) 2.9 Vrms, (f) 3.3 Vrms, (g) 3.7 Vrms, (h) 4.8 Vrms, and (i) 5.9 Vrms.

can be eliminated with proper alignment and filling techniques. The experiments show that nanotubes can form submicron pixels in a liquid crystal media and these experiments will lay down the foundation for making submicron pixels and active back planes using nanotubes electrodes.

6. CONCLUSIONS

The paper presented the simulation and fabrication of interdigitated rows of carbon nanotube electrodes to address a liquid crystal media. Finite Element Method (FEM) modeling of the nanotube geometry was performed to find suitable device geometry from the static electric field study. The interdigitated nanotube electrodes were fabricated using e-beam lithography and PECVD techniques. It was observed that nanotubes interact with liquid crystal and showed a different colour just around the interdigitated electrodes compared to dark colour of the liquid crystal without any nanotube electrodes between crossed

polarizer and analyzer. The electro optic experiments showed that nanotubes can be used for realizing micron and submicron pixels as well as active nanotube based back planes. The device can also be used for precise beam steering where each row in the interdigitated pattern can be given different voltages to create a micron saw-tooth periodic phase profile, characteristic of a blazed grating.

ACKNOWLEDGMENT

This work was partly funded under the Nokia-Cambridge Strategic Partnership in Nanoscience and Nanotechnology (Energy Programme).

REFERENCES

1. Baughman, R. H., A. A. Zakhidov, and W. A. de Heer, "Carbon nanotubes — The route toward applications," *Science*, Vol. 297, 787–792, August 2, 2002.
2. Milne, W. I., K. B. K. Teo, M. Chhowalla, G. A. J. Amaratunga, S. B. Lee, D. G. Hasko, H. Ahmed, O. Groening, P. Legagneux, L. Gangloff, J. P. Schnell, G. Pirio, D. Pribat, M. Castignolles, A. Loiseau, V. Semet, and V. T. Binh, "Electrical and field emission investigation of individual carbon nanotubes from plasma enhanced chemical vapour deposition," *Diamond and Related Materials*, Vol. 12, 422–428, 2003.
3. Wang, X. Q., M. Wang, H. L. Ge, Q. Chen, and Y. B. Xu, "Modeling and simulation for the field emission of carbon nanotubes array," *Physica E: Low-dimensional Systems and Nanostructures*, Vol. 30, 101–106, 2005.
4. Deuk-Seok, C., S. H. Park, H. W. Lee, J. H. Choi, S. N. Cha, J. W. Kim, J. E. Jang, K. W. Min, S. H. Cho, M. J. Yoon, J. S. Lee, C. K. Lee, J. H. Yoo, K. Jong-Min, J. E. Jung, Y. W. Jin, Y. J. Park, and J. B. You, "Carbon nanotube electron emitters with a gated structure using backside exposure processes," *Applied Physics Letters*, Vol. 80, 4045–4047, 2002.
5. Chen, Y., C. Liu, and Y. Tzeng, "Carbon-nanotube cold cathodes as non-contact electrical couplers," *Diamond and Related Materials*, Vol. 12, 1723–1728, 2003.
6. Wilkinson, T. D., X. Wang, K. B. K. Teo, and W. I. Milne, "Sparse multiwall carbon nanotube electrode arrays for liquid-crystal photonic devices," *Advanced Materials*, Vol. 20, 363–366, 2008.

7. Butt, H., R. Ranjith, T. D. Wilkinson, and G. A. J. Amaratunga, "Electromagnetic modeling of multiwalled carbon nanotubes as nano-rod electrodes for optimizing device geometry in a nanophotonic device," *IEEE Transactions on Nanotechnology*, Vol. 10, No. 3, 2011.
8. Qing, D., R. Ranjith, B. Haider, W. Kanghee, W. Xiaozhi, D. W. Timothy, and A. Gehan, "Transparent liquid-crystal-based microlens array using vertically aligned carbon nanofiber electrodes on quartz substrates," *Nanotechnology*, Vol. 22, 115201, 2011.
9. Rajasekharan, R., C. Bay, Q. Dai, J. Freeman, and T. D. Wilkinson, "Electrically reconfigurable nanophotonic hybrid grating lens array," *Applied Physics Letters*, Vol. 96, 233108-3, 2010.
10. COMSOL, "COMSOL multiphysics," 3.3a Ed, p. FEMLAB is registered trademark of COMSOL, 2007.
11. Rajasekharan-Unnithan, R., H. Butt, and T. D. Wilkinson, "Optical phase modulation using a hybrid carbon nanotube-liquid-crystal nanophotonic device," *Opt. Lett.*, Vol. 34, 1237–1239, 2009.
12. Ye, M., B. Wang, and S. Sato, "Liquid crystal lens with focus movable in focal plane," *Optics Communications*, Vol. 259, 710–722, 2006.
13. Wang, B., M. Ye, and S. Sato, "Liquid crystal lens with focal length variable from negative to positive values," *IEEE Photonics Technology Letters*, Vol. 18, 79–81, 2006.
14. Rajasekharan-Unnithan, R., "Nanophotonic devices based on carbon nanotubes and liquid crystals," *Engineering*, University of Cambridge, Cambridge, 2011.